Frequency based strategy for hybrid-powered unmanned aerial vehicle

T. Pavot[1]*, M. Lefebvre[1], R. Kiefer[1], T. Mesbahi[1], E. Laroche[2]
[1]INSA Strasbourg, ICube laboratory UMR7357, 24 Boulevard de la Victoire, Strasbourg, France
[2] Strasbourg University, 3-5 rue de l'université, Strasbourg, France

ABSTRACT

Recent developments of different energy sources such as fuel cells (FC), batteries and supercapacitors (SC) show great potential to increase the lifetime and endurance of electric unmanned aerial vehicles (UAV). By knowing the flight cycle, it is possible to optimize the flight time by playing on the advantages and disadvantages of each source. This paper proposes to evaluate the influence of the cutoff frequency to be chosen in order to optimize the lifetime of the hybrid system. To resolve this, a frequency strategy allowing to have a variable cut-off frequency according to the energy stored by the supercapacitors (SC) is developed.

1 INTRODUCTION

From 2017 to 2020, the INSA Strasbourg team developed the Stork drone (Fig.1) as part of the European INTERREG ELCOD project (Endurance Low COst Drone[1]). This drone has been designed to perform long endurance flights for various types of missions, including the measurement of air pollutants. It has a maximum take-off weight of 25 kg (MTOW = 25 kg) and a wingspan of 5 m. This UAV is powered by a hybrid source based on a hydrogen fuel cell associated with a lithium polymer (LiPo) battery. From the tests carried out, the hybridization system of type "all or nothing" proposed by the majority of the manufacturers shows that it is far from being optimal and has limitations.

The objective of this work is to propose a structure and a control of the different hybridization sources in order to optimize the energy management and to improve their lifetime. The Stork UAV and its flight cycle will be used as an typical application to meet the objective of improving energy management within a long endurance UAV by hybridizing three different sources [1]. : a 1000 W PEMFC fuel cell (FC) [2], a LiPo battery and supercapacitors (SC).

This paper will focus on the implementation of a frequency-based power management strategy for hybridization. First, hybridization and sources will be introduced. Then, the strategy with a fixed cutoff frequency will then be discussed with a comparison between simulation and test bench implementation. Finally, the strategy based on a variable cutoff frequency depending on the SC state of charge (SoC) will be compared to the use of a fixed frequency in simulation.

*Email address(es): thomas.pavot@insa-strasbourg.fr
[1]www.elcod.eu

Figure 1: Stork UAV

2 HYBRIDIZATION STRUCTURES

The three sources (FC, SC and batteries) can be classified by their energy density according to their power density. This graph is called the Ragone diagram (Fig.2).

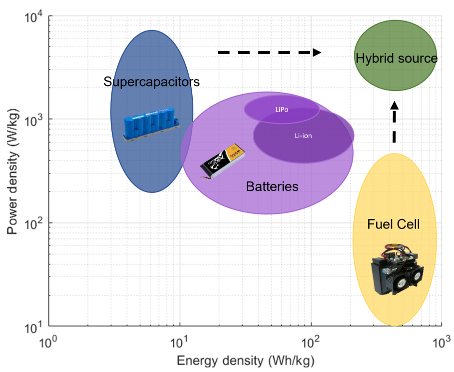

Figure 2: Ragone plot

The interest of creating a hybrid system by associating these three sources, is to allow the system to have a high energy density while ensuring high power density. In other words, the FC is present to ensure endurance while the SCs ensure power variations. The presence of the battery in our case ensures an auxiliary role by making it possible to bring the surplus of power during the phase of takeoff, the supply of the system to the starting and to bring a safety in the event of breakdown. The hybridization aims to extend the lifetime of the sources while ensuring the maximum autonomy with the constraints of mass and volume inerrant to the drone. The first triple hybridization was performed in 2018. It was a passive hybridization [3].The literature proposes different hybridization architectures depending on the configuration [4].

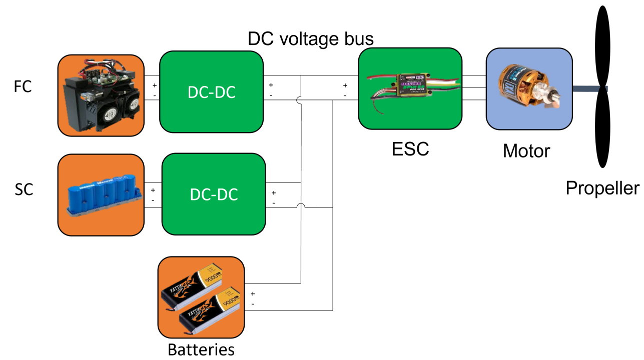

Figure 3: Semi-active architecture

The basic architecture chosen for our system is a so-called semi-active structure (Fig.3). It allows the control of the FC, and the SC by the control of two DC-DC converters. As for the battery, it ensures a stable voltage on the DC bus. This architecture allows the battery to provide additional energy to the system during the entire ascent phase. This surplus of energy cannot be provided by the FC and the SC limited by the converters used.

The control of these sources will be done by the activation of two DC-DC converters able to adapt the voltages and to transfer the powers from a source of energy to another according to the energy needs of the drone. This system uses a minimum of converters thus reducing the number of components and consequently the mass and the price.

3 SOURCES AND DC-DC CONVERTERS

3.1 Fuel cell (FC)

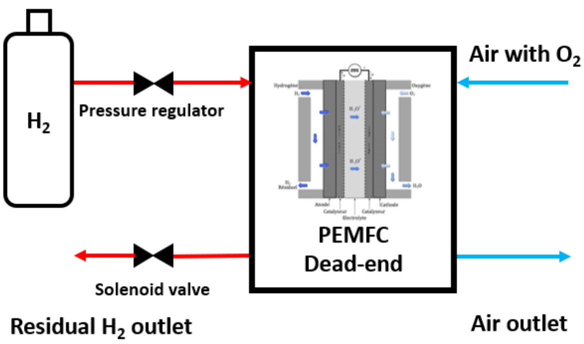

Figure 4: PEMFC dead-end

Table 1: Aerostack PEM fuel cells HES energy system

Specification	Value
Number of cells	50
Max voltage	50V
Voltage at 1000W	33V
Rated power	1000 W
Weight	2182 g
Max H−2 flow rate	15 slpm @ 1000 W
H−2 pressure	0.55 to 0.77 bar
Peak Efficiency	50%
Humidification	Self-humidified

The FC used is a PEMFC (Proton Exchange Membrane Fuel Cell) of the dead-end type (Fig.4). This type of FC uses as reagent dihydrogen stored at high pressure (300 bars) in an on-board tank which will react with dioxygen present in the air. The dead-end type means that the anodic conduit where the dihydrogen transits is closed [5].

This technology is the lightest and most compact of the different FC technologies. It is suitable for an on-board application in a drone. Its only limit is the flight altitude since the reaction needs a sufficient concentration of oxygen to work. A limit of 3000 m is given by the manufacturer of the FC.

The evolution of the voltage of a PEMFC presents a slow dynamic of a few seconds depending in particular on the humidity of the membrane[6]. The strong variations of current lead to variations of voltage causing a wear of the FC. The literature shows that control with low dynamics decreases the degradation of PEMFCs [7].

The FC used is a 1000W PEMFC aerostack (Table.1) from HES energy system associated to a 6L tank able to contain dihydrogen at 300bar.

3.2 LiPo batteries

LiPo lithium polymer batteries are widely used in electronic devices (smartphones and laptops) and in model making because of their high discharge current and their mass comparable to other types of lithium batteries. However, they are more expensive and have a shorter lifetime compared to lithium-ions which are present in electric vehicles.

The literature clearly shows that current and temperature are the main causes of degradation, whether it is due to time or use. The wear caused will be seen on a decrease of the storage capacity and on the maximum power that can provide the battery [8].

Just like the PEMFC, the LiPo batteries deteriorate with the variations of current and temperature [9, 10].

The batteries used during the flight of the drone are LiPo 9000mAh batteries with a nominal voltage of 14.8V (Table.2). They are associated in series in order to have approximately 32V.

Table 2: Tattu LiPo Batteries

Specification	Value
Number of cells	4
Nominal voltage	15.6 V
Weight	809 g
Max current	225 A

3.3 Supercapacitors (SC)

Supercapacitors are electrical dipoles capable of storing a small amount of energy by rapidly charging and discharging. The use of SCs is growing rapidly, they are used in many applications (hybrid vehicles, military warheads, telecommunication, laser technology and photovoltaic panels) [11] to supplement a main power source (often batteries).

The SCs used here are oversized for the application because they are removed off the shelf. It is a block of 6 Maxwell SCs in series with a capacity of 58F (Table.3).

Table 3: Maxwell 16V 58F SC

Specification	Value
Part Number	BMOD0058 E016 B02
Capacity	58F
Max current	12 A continuous & 200 A burst
Max nominal voltage	16 V
Weight	630 g
Max current	225 A

3.4 DC-DC converters

The two converters have an architecture composed of two mosfets in half bridge controlled in reverse associated with a coil and a capacitor. The BuckBoost topology (Fig.5) allows to make these converters unidirectional in voltage and bidirectional in current. The switching frequency used is 20kHz and they are limited to 500 W on the test bench.

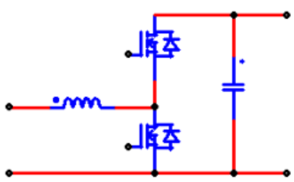

Figure 5: DC-DC converters

4 Hybridization strategies

To operate these converters efficiently, the EMS (Energy Management Strategy) is responsible for ensuring that the energy mix is right for the drone's needs at all times, while maximizing the autonomy and lifetime of the energy sources. The design of an EMS is built by defining a reference flight cycle, objectives (low energy consumption, lifetime ...) and operating criteria (power sources, limits ...). Once this framework is defined, the literature proposes several categories of EMSs [12] for source hybridization :

- Strategies defined by rules (Rule-Based) [13, 14]
- Intelligent strategies based on neural networks or fuzzy logic (Inteligent-Based) [15, 16]
- Optimization strategies (Optimization-Based) [17, 18]
- Other strategies such as frequency cutting [19, 20]

In this paper, the frequency method (Fig.6) has been chosen since it requires low computational power and can easily be implemented in a UAV. This method also allows to respect a sufficiently slow response time in order not to damage the FC by leaving the strong dynamics to the SC. This EMS strategy limits the current variations provided by the FC thus reducing its wear and extending its life.

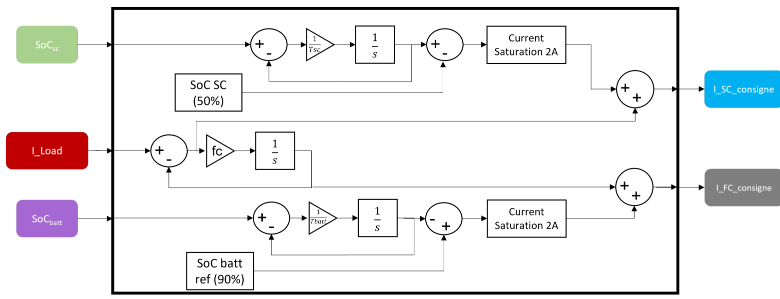

Figure 6: EMS : cut-off frequency

In order to distinguish low frequencies from high frequencies, a first cut-off frequency fc must be determined. The value of $fc = 0.5Hz$ was chosen to allow the fuel cell to respond to the maximum step that the system can undergo. This cut-off frequency also avoids discharging the SC too much during this same step by losing about 10% of its initial state of charge (SoC). This value of cutoff frequency was used as a basis for the continuation by using it on the model and on the test bench. The rest of the article will discuss how to determine the right cutoff frequency for the system.

The second role of the EMS is to maintain a level of SoC for the battery and for the SC. The system will try to maintain the SoC of SC at 50% with a slow feedback loop. This value allows the SC to be able to handle current variations without discharging or overloading itself. In the same way, the battery will be maintained at a SoC of 80%. The battery will be discharged during the phase of takeoff in order to provide the surplus of necessary energy (approximately 1000W). Then, at the time of the cruise flight, the EMS will have for role to recharge then to maintain the SoC of the battery. The value of 80% ensures an autonomy in case of failure of about 30 minutes with the current dimensioning.

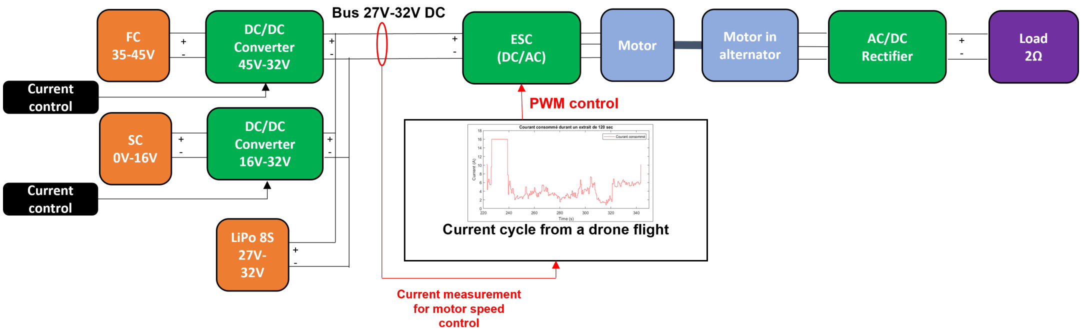

Figure 7: Diagram of the test bench

5 NUMERICAL MODELING AND EXPERIMENTAL VALIDATION

To test the EMS, a numerical simulation was performed using the Matlab Simulink software. The modeling of each of the three sources is based on equivalent electrical models. These models easily represent the dynamic behaviors and require a low computation time [21, 22]. Concerning the converters, the modeling is made from an average model not taking into account the chopping caused by the switching of the transistors. These converters are controlled in current with a simple regulation loop using PI (Proportional Integrator) correctors. These models put end to end allowed to have a first representation of the complete functioning of the chosen hybridization architecture.

In order to validate the modeling, a test bench has been realized allowing to perform the same tests. The test bench is represented by its functional diagram on the Fig.7. It is controlled by a Dspace interface (RTI1104) performing the acquisition of voltages and currents and the sending of cyclic control reports to the converters. The load is composed of the ESC (Electronic Speed Controler) and the drone's motor, which are coupled to a second motor/alternator that acts as a brake, dissipating energy through a resistor. The ESC control simulates a current cycle from a real flight of the drone at the nominal operating point of the cruise flight (450 W) to obtain a realistic behavior.

To make the modeling and test bench work, a reference flight cycle that drives the motor must be defined. The EL-COD project has made it possible to carry out flights with the Stork drone allowing to have a realistic current cycle. The selected test is an extract of 120 sec (Fig.8 (a)) of a flight which lasted 30 min including a phase of rise and a phase of flight of cruising. To adapt to the current limit of the bench, the current cycle was divided by 3 and saturated at 16A. These same limitations were applied to the modeling.

The Fig.8 allows to compare the results of the modeling with the experimental test. In Fig.8 (b)(c)(d), the curves show the currents from the simulation compared to those obtained during the experimental test. These are the currents from

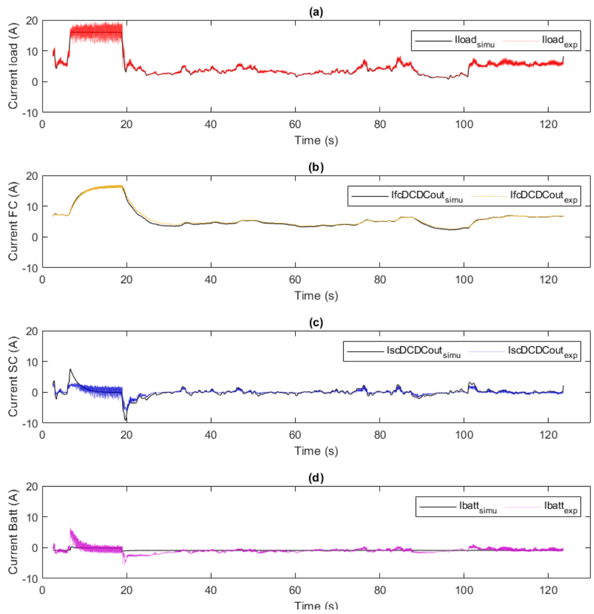

Figure 8: Illustration showing a comparison between the test bench results and the proposed model currents. (a): load current. (b): FC current. (c): SC current. (d): Battery currents.

the FC, SC and batteries (yellow, blue and purple respectively). The blue (IscDCDCout) and yellow (IfcDCDCout) curves represent the output current of each converter. The curves from the simulation are in dark line while the curves from an experimental test are in colored line. The frequency strategy (here with $fc = 0.5Hz$) smoothes the current supplied by the fuel cell. The SC fulfills its role by reacting to fast current demands.

The curves are consistent between the simulation and the experimental. However, during the current draw caused by the load at about 6 sec, we note a difference between the simulation and the experimental test for the battery and the SC. Indeed, in simulation, the battery delivers a current close to 0A, but during the test it compensates the high frequency variations which should be filled by the SC. The blue curve of the test shows that the SC does not manage to follow the set point during the current call. This is for the moment a defect in the operation of the converter. Apart from this fault, the model corresponds to the experimental test. This test allows to validate the operation and now allows to go further in the modeling by testing new variants of the frequency method as EMS.

6 FREQUENCY METHOD: FIXED CUT-OFF FREQUENCY VS VARIABLE CUT-OFF FREQUENCY

The frequency method gives good results by having a cut-off frequency adapted to its system. It is however difficult to determine the best value allowing not to discharge or overload the SC while keeping a sufficiently slow response time not to damage the FC without knowing the flight cycle in advance. The method proposed here allows to vary the cutoff frequency according to the SoC of the SC.

6.1 Theory

The EMS concept, entails delivering the low frequency components of power to the energy source (FC) and the high frequency components to the power source (SCs). A low-pass filter with a variable cut-off frequency f_c is used to achieve this distribution. This last one has an immediate impact on the power restrictions imposed to the FC. The proposed approach in this paper consists on adjusting the cut-off frequency of the filter in real time based on the SoC_{sc} value and reacting fast to load variations. The use of a variable frequency means that there is a high and a low limit to the frequencies used such as $fc_{Hlim} > fc_{Llim}$. These limits are calculated to avoid damaging the SC while maximizing its use. To set these limits, the calibration is done by applying the highest current step that the system can undergo with a fixed cutoff frequency. Having an initial SoC of 50%, the SC has to be able to charge or discharge by 25% to the maximum while undergoing the step. This allows to keep a good efficiency of use of the SC. By respecting this criterion, the minimum cutoff frequency (fc_{Llim}) is 0.125Hz for our system. Conversely, when the SoC of the SC is close to full discharge or overload, it should not undergo a variation of the SoC greater than 5% of its value. This criterion allows in our case to have a high cutoff frequency (fc_{Hlim}) at 1 Hz.

$$fc(t) = (F_{cHlim} - F_{cLlim}) \cdot e^{-5 \cdot SoC(t)} + F_{cLlim} \quad (1)$$

The equation (Eq.1) allowing to link the SoC to the cut-off frequency while taking into account the two previous limits is an exponential equation. This type of equation allows to keep an important dynamics of the system when the SoC evolves around the reference value (50%) while when it moves away enough from this value, the SC becomes much less reactive. The equation (Eq.1) changes if the SC has to charge or discharge. When the SC discharges $SoC(t)$ becomes $1 - SoC(t)$.

6.2 Result and analysis of the simulation

In order to compare the two frequency methods. Three fixed frequencies were chosen. The first is 0.125Hz corresponding to F_{cLlim}. It is the value which makes it possible to completely discharge our SC at the time of the current step undergone at takeoff. This value is problematic because the efficiency of the SC when its SoC drops below 25% is increasingly worse. Indeed to maintain the power at the output of the converter, the current at the output of the SC will increase considerably causing losses by Joule effect. The second value of 1Hz selected corresponds to the F_{cHlim}. This value is too slow and does not allow the SC to be used to its full potential and causes significant variations in the current supplied by the FC. The third and last value is 0.3Hz allowing to have a discharge of the SoC of 25%. This is the fixed cutoff frequency that seems the most optimal on our system for the 120 sec test.

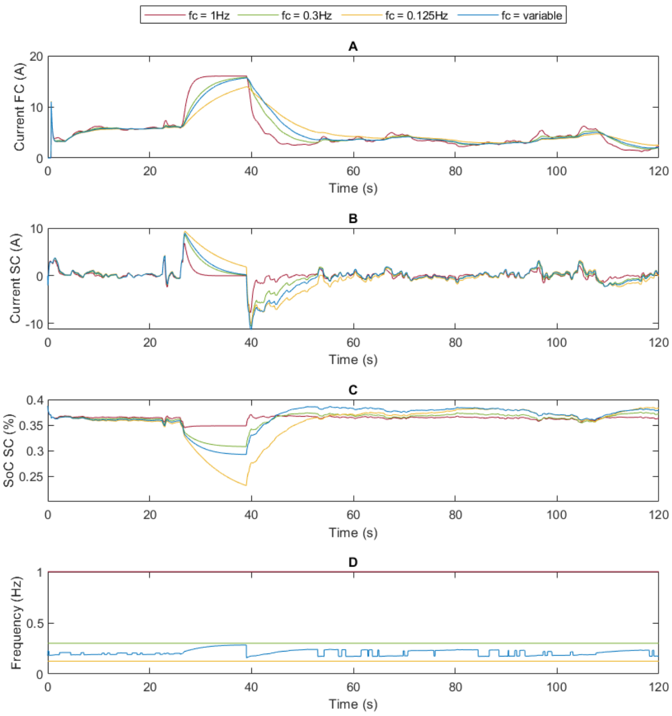

Figure 9: Illustration showing a comparison between different fixed and variable cut-off frequencies, (a): FC current. (b): SC Current. (c): Battery current. (d): SoC of SC. (e): Frequency.

The Fig.9 shows the current curves of each source and the evolution of the SoC of the SC and the cutoff frequency on the 120 sec test. It is interesting to note that the variable frequency allows to have a dynamic close to the fixed frequency of 0.125Hz when the SoC of the SC is close to 0.5 while respecting the discharge during the step of approximately 25% as that of 0.3Hz. These advantages make it possible to better exploit the dynamics of the SC by leaving a slow response time for the FC. The current variations of the FC are therefore lower with a low cut-off frequency allowing an extension of the lifetime. (Fig.9, A). From a safety point of view, the equation allows to avoid at any time to have the SoC of the SC approaching 0 or 1 (Fig.9, B and C) with an approximate setting of the limits. The variable frequency allows the system to maintain a higher dynamic range of the SC without the risk of damaging it with too much charge or discharge.

7 CONCLUSION

In this study, we've first presented the Stork UAV with its power system composed of SC, FC and batteries. Following that, we developed a model of our system and an experimental test bench. The tests conducted allowed us to validate the model with a fixed frequency strategy. We provided an approach to determining the low-pass filter EMS parameters and tuning fc using the SC's SoC. This approach enables the SCs to run with high dynamics while avoiding a SoC_{sc} of 25% or below where efficiency is limited. As a result, this solution should extend the FC's life. In addition to that, this technique allows to better protect the SCs from overcharging/discharging. The future prospects of this work include the search for reliable indicators to prove that the proposed solution brings benefits for the autonomy and the lifetime of the UAV. The comparison with new EMS algorithms such as robust control or optimal control will be studied in order to provide a comparison with the frequency method developed here.

ACKNOWLEDGEMENTS

The authors thank ICUBE laboratory from Strasbourg University and INSA Strasbourg for funding this study.

REFERENCES

[1] M. Boukoberine, Z. Zhou, and M. Benbouzid. A critical review on unmanned aerial vehicles power supply and energy management: Solutions, strategies, and prospects, dec 2019.

[2] Z. F. Pan, L. An, and C. Y. Wen. Recent advances in fuel cells based propulsion systems for unmanned aerial vehicles, apr 2019.

[3] A. Gong and D. Verstraete. Flight Test of a Fuel-Cell / Battery / Supercapacitor Triple Hybrid. *31st Congress of the International Council of the Aeronautical Sciences*, (September):1–10, 2018.

[4] B. Wang, D. Zhao, W. Li, Z. Wang, Y. Huang, Y. You, and S. Becker. Current technologies and challenges of applying fuel cell hybrid propulsion systems in unmanned aerial vehicles. *Progress in Aerospace Sciences*, 116(May), 2020.

[5] S. Abbou. *Phénomènes locaux instationnaires dans les piles à combustible à membrane (PEMFC) fonctionnant en mode bouché (dead-end).* PhD thesis, 2015.

[6] Ph Moçotéguy, F. Druart, Y. Bultel, S. Besse, and A. Rakotondrainibe. Monodimensional modeling and experimental study of the dynamic behavior of proton exchange membrane fuel cell stack operating in dead-end mode. *Journal of Power Sources*, 167(2):349–357, may 2007.

[7] E. Pahon, S. Jemei, N. Steiner, and D. Hissel. Effect of load cycling on the performance of fuel cell stacks. *2019 IEEE Vehicle Power and Propulsion Conference, VPPC 2019 - Proceedings*, 2019.

[8] E. Iglesias. Étude du vieillissement des batteries lithium-ion dans les applications "véhicule électrique" : Combinaison des effets de vieillissement calendaire et de cyclage. Technical report, 2017.

[9] R. Xiong, Y. Pan, W. Shen, H. Li, and F. Sun. Lithium-ion battery aging mechanisms and diagnosis method for automotive applications: Recent advances and perspectives, oct 2020.

[10] C. Vidal, O. Gross, R. Gu, P. Kollmeyer, and A. Emadi. XEV Li-Ion Battery Low-Temperature Effects-Review. *IEEE Transactions on Vehicular Technology*, 68(5):4560–4572, may 2019.

[11] W. Raza, F. Ali, N. Raza, Y. Luo, K. Kim, J. Yang, S. Kumar, A. Mehmood, and E. Kwon. Recent advancements in supercapacitor technology, oct 2018.

[12] T. Lei, Z. Yang, Z. Lin, and X. Zhang. State of art on energy management strategy for hybrid-powered unmanned aerial vehicle, jun 2019.

[13] B. Lee, S. Kwon, P. Park, and K. Kim. Active power management system for an unmanned aerial vehicle powered by solar cells, a fuel cell, and batteries. *IEEE Transactions on Aerospace and Electronic Systems*, 50(4):3167–3177, 2014.

[14] Y. Han, W. Chen, and Q. Li. Energy Management Strategy Based on Multiple Operating States for a Photovoltaic/Fuel Cell/Energy Storage DC Microgrid. 2017.

[15] X. Zhang, L. Liu, Y. Dai, and T. Lu. Experimental investigation on the online fuzzy energy management of hybrid fuel cell/battery power system for UAVs. *International Journal of Hydrogen Energy*, 43(21):10094–10103, 2018.

[16] H. Khayyam and A. Bab-Hadiashar. Adaptive intelligent energy management system of plug-in hybrid electric vehicle. *Energy*, 69:319–335, 2014.

[17] V. Larsson, L. Johannesson, and B. Egardt. Analytic solutions to the dynamic programming subproblem in hybrid vehicle energy management. *IEEE Transactions on Vehicular Technology*, 64(4):1458–1467, 2015.

[18] P. García, J. P. Torreglosa, L. M. Fernández, and F. Jurado. Viability study of a FC-battery-SC tramway controlled by equivalent consumption minimization strategy. *International Journal of Hydrogen Energy*, 37(11):9368–9382, 2012.

[19] H. Xiaoliang, T. Hiramatsu, and H. Yoichi. Energy management strategy based on frequency-varying filter for the battery supercapacitor hybrid system of Electric Vehicles. *World Electric Vehicle Journal*, 6(3):623–628, 2013.

[20] J. Snoussi, S. Ben Elghali, M. Benbouzid, and M. Mimouni. Auto-adaptive filtering-based energy management strategy for fuel cell hybrid electric vehicles. *Energies*, 11(8):1–20, 2018.

[21] F. Belhaj, H. El Fadil, Z. El Idrissi, A. Intidam, M. Koundi, and F. Giri. New equivalent electrical model of a fuel cell and comparative study of several existing models with experimental data from the PEMFC nexa 1200 W. *Micromachines*, 12(9), 2021.

[22] Y. Ghoulam, T. Paul, T. Mesbahi, and S. Durand. Modeling, Identification and Simulation of Hybrid Battery/Supercapacitor Storage System Used in Vehicular Applications. *6th International Conference on Electric Vehicular Technology 2019*, (November):156–162, 2019.